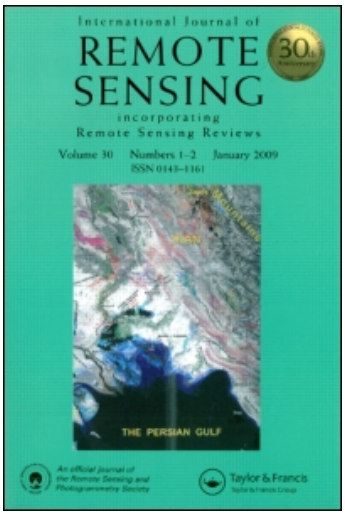

International Journal of Remote Sensing
Publication details, including instructions for authors and subscription information:
http://www.informaworld.com/smpp/title~content=t713722504

Landscape as a continuum: an examination of the urban landscape structures and dynamics of Indianapolis City, 1991-2000, by using satellite images

Qihao Weng [a]; Dengsheng Lu [b]
[a] Center for Urban and Environmental Change, Department of Geography, Geology, and Anthropology, Indiana State University, Terre Haute, IN, USA [b] School of Forestry and Wildlife Sciences, Auburn University, Auburn, AL, USA

Online Publication Date: 01 January 2009

To cite this Article Weng, Qihao and Lu, Dengsheng(2009)'Landscape as a continuum: an examination of the urban landscape structures and dynamics of Indianapolis City, 1991-2000, by using satellite images',International Journal of Remote Sensing,30:10,2547 — 2577

To link to this Article: DOI: 10.1080/01431160802552777

URL: http://dx.doi.org/10.1080/01431160802552777

International Journal of Remote Sensing
Vol. 30, No. 10, 20 May 2009, 2547–2577

Taylor & Francis
Taylor & Francis Group

Landscape as a continuum: an examination of the urban landscape structures and dynamics of Indianapolis City, 1991–2000, by using satellite images

QIHAO WENG*† and DENGSHENG LU‡
†Center for Urban and Environmental Change, Department of Geography, Geology, and Anthropology, Indiana State University, Terre Haute, IN, USA
‡School of Forestry and Wildlife Sciences, Auburn University, Auburn, AL, USA

(*Received 11 October 2007; in final form 1 February 2008*)

The majority of the vast literature on remote sensing of urban landscapes has adopted a 'hard classification' approach, in which each image pixel is assigned a single land use and land cover category. Owing to the nature of urban landscapes, the confusion between land use and land cover definitions and the constraints of widely applied medium spatial resolution satellite images, high classification accuracy has been difficult to achieve with the conventional 'hard' classifiers. The prevalence of the mixed pixel problem in urban landscapes indicates a crucial need for an alternative approach to urban analyses. Identification, description and quantification, rather than classification, may provide a better understanding of the compositions and processes of heterogeneous landscapes such as urban areas. This study applied the Vegetation–Impervious Surface–Soil (V-I-S) model for characterizing urban landscapes and analysing their dynamics in Indianapolis, USA, between 1991 and 2000. To extract these landscape components from three dates of Landsat Thematic Mapper/Enhanced Thematic Mapper Plus (TM/ETM+) images in 1991 1995 and 2000, we used the technique of linear spectral mixture analysis (LSMA). These components were further classified into urban thematic classes, and used for analysis of the landscape patterns and dynamics. The results indicate that LSMA provides a suitable technique for detecting and mapping urban materials and V-I-S component surfaces in repetitive and consistent ways, and for solving the spectral mixing of medium spatial resolution satellite imagery. The reconciliation between the V-I-S model with LSMA for Landsat imagery allowed this continuum landscape model to be an alternative, effective approach to characterizing and quantifying the spatial and temporal changes of the urban landscape compositions in Indianapolis from 1991 to 2000. It is suggested that the model developed in this study offers a more realistic and robust representation of the true nature of urban landscapes, as compared with the conventional method based on 'hard classification' of satellite imagery. The general applicability of this continuum model, especially its spectral, spatial and temporal variability, is discussed.

1. Introduction

Urban landscapes are typically a complex combination of buildings, roads, parking lots, sidewalks, gardens, cemeteries, soil, water, and so on. Each of the urban

*Corresponding author. Email: qweng@indstate.edu

International Journal of Remote Sensing
ISSN 0143-1161 print/ISSN 1366-5901 online
http://www.tandf.co.uk/journals
DOI: 10.1080/01431160802552777

component surfaces exhibits unique radiative, thermal, moisture and aerodynamic properties, and relates to its surrounding site environment to create the spatial complexity of ecological systems (Oke 1982). To understand the dynamics of patterns and processes and their interactions in heterogeneous landscapes such as urban areas, we need to quantify the spatial pattern of the landscape and its temporal changes (Wu *et al.* 2000). It is therefore necessary (1) to have a standardized method to define these component surfaces, and (2) to detect and map them in repetitive and consistent ways, so that a global model of urban morphology may be developed, and their changes over time can be monitored and modelled (Ridd 1995).

Remote sensing technology has been widely applied in urban land use, land cover classification and change detection. However, it is rare that a classification accuracy greater than 80% can be achieved by using per-pixel classification (so-called 'hard classification') algorithms (Mather 1999, p. 10). The low accuracy of land use/land cover (LU/LC) classification in urban areas is largely attributed to the mixed pixel problem, where several types of LU/LC are contained in one pixel. The mixed pixel problem results from the fact that the scale of observation (i.e. pixel resolution) fails to correspond to the spatial characteristics of the target (Mather 1999). Therefore, the 'soft'/fuzzy approach of LU/LC classifications has been applied, in which each pixel is assigned a class membership of each LU/LC type rather than a single label (Wang 1990). Nevertheless, as Mather (1999) pointed out, neither 'hard' nor 'soft' classification is an appropriate tool for the analysis of heterogeneous landscapes. Both Ridd (1995) and Mather (1999) maintained that identification, description and quantification, rather than classification, should be applied to provide a better understanding of the compositions and processes of heterogeneous landscapes such as urban areas.

Ridd (1995) proposed a major conceptual model for remote sensing analysis of urban landscapes: the vegetation–impervious surface–soil (V-I-S) model (figure 1). The V-I-S model assumes that land cover in urban environments is a linear combination of three components: vegetation, impervious surface, and soil. Ridd suggested that this model could be applied to spatial–temporal analyses of urban morphology, biophysical and human systems. Although urban land use information may be more useful in socioeconomic and planning applications, biophysical information that can be directly derived from satellite data is more suitable for describing and quantifying urban structures and processes (Ridd 1995). The V-I-S model was developed for Salt Lake City, Utah, but has been tested in other cities. Ward *et al.* (2000) applied a hierarchical unsupervised classification approach to a Landsat Thematic Mapper (TM) image in southeast Queensland, Australia, based on the V-I-S model. An adjusted overall accuracy of 83% was achieved. Madhavan *et al.* (2001) used an unsupervised classifier to classify TM images in Bangkok, Thailand, with the V-I-S model, and found it to be useful for improving classification and analysis of change trends. Similar to the Ward *et al.* approach, Setiawan *et al.* (2006) applied a V-I-S-based hieratical procedure to classify a Landsat TM image of Yogyakarta, Indonesia, and found its accuracy was 27% better than the maximum likelihood algorithm. All of these studies used the V-I-S model as the conceptual framework to relate urban morphology to medium-resolution satellite imagery, but 'hard classification' algorithms were applied. However, the problem of mixed pixels cannot be solved by this method, and the analysis of urban landscapes was still based on 'pixels' or 'pixel groups'.

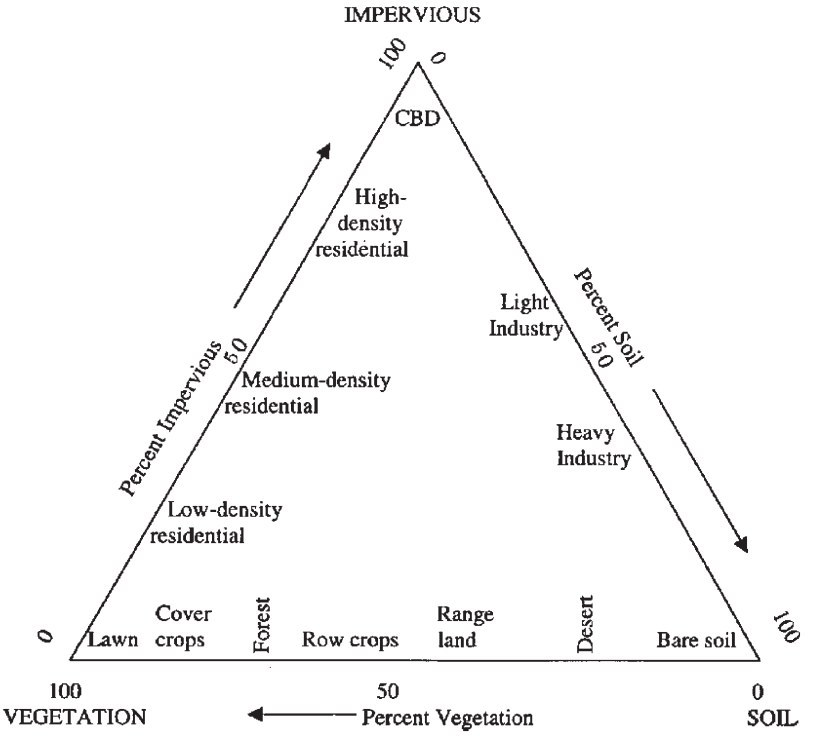

Figure 1. The Vegetation–Impervious surface–Soil (V-I-S) model illustrating the characteristics of urban landscapes (Ridd 1995).

Linear spectral mixture analysis (LSMA) is another approach that can be used to handle the mixed pixel problem, besides the fuzzy classification. Instead of using statistical methods, LSMA is based on physically deterministic modelling to unmix the signal measured at a given pixel into its component parts, called endmembers (Adams *et al.* 1986, Boardman 1993, Boardman *et al.* 1995). Endmembers are recognizable surface materials that have homogeneous spectral properties all over the image. LSMA assumes that the spectrum measured by a sensor is a linear combination of the spectra of all components within the pixel (Boardman 1993). Because of its effectiveness in handling spectral mixture problems and its ability to provide continuum-based biophysical variables, LSMA has been widely used in: (1) the estimation of vegetation cover (Asner and Lobell 2000, McGwire *et al.* 2000, Small 2001, Weng *et al.* 2004, Lee and Lathrop 2005), (2) impervious surface estimation and/or urban morphology analysis (Phinn *et al.* 2002, Wu and Murray 2003, Rashed *et al.* 2003, Wu *et al.* 2005, Lu and Weng 2006*a*,*b*), (3) vegetation or land cover classification (Adams *et al.* 1995, Cochrane and Souza 1998, Aguiar *et al.* 1999, Lu and Weng 2004), and (4) change detection (Rashed *et al.* 2005, Powell *et al.* 2007). However, with a few exceptions, these studies have focused on technical specifics and on the examination of the effectiveness of LSMA. Only a few studies have explicitly adopted the V-I-S model as the conceptual model to explain urban land cover patterns (Phinn *et al.* 2002, Wu and Murray 2003, Wu *et al.* 2005, Lu and Weng 2006*a*,*b*, Powell *et al.* 2007), while others have used it implicitly (Rashed *et al.* 2003, 2005). Rashed *et al.* (2005) and Powell *et al.* (2007) are the only research attempts to examine urban land cover 'change' with the V-I-S model. Rashed *et al.*

(2005) assessed changes between landscape components aggregated to census tracts in Cairo, Egypt, but determination of the thresholds of change may be problematic because they may vary from image to image. Powell *et al.* (2007) identified the stages of urban development by selecting four neighbourhoods from an image of Manaus, Brazil that did not involve change detection from multitemporal satellite images.

Having realized that the V-I-S model may be used as a method to define standardized urban landscape components, along with LSMA as a remote sensing technique to estimate and map them in repetitive and consistent ways, it is necessary to reconcile them to develop a global model of urban morphology. The objective of this paper was to apply the V-I-S model to an examination of the urban land cover patterns and temporal dynamics in Indianapolis, Indiana, USA, from 1991 to 2000. Landsat TM/Enhanced Thematic Mapper Plus (ETM+) multitemporal satellite images from 1991, 1995 and 2000 were used to extract the landscape components using the technique of LSMA. The specific aims of this research were: (1) to apply LSMA to derive V-I-S components to characterize the urban morphology of Indianapolis in three observation times; (2) to analyse spatial–temporal changes of the urban morphology by assessing changes in the V-I-S components; and (3) to examine intra-urban variations in landscape structures by comparative analysis of the V-I-S compositions and dynamics among the nine townships in the city. Based on this case study, this paper further investigated the general applicability of the V-I-S model as a continuum landscape model.

2. Urban landscape analysis with remote sensing

2.1 *Current challenges*

2.1.1 Urban materials, land cover, and land use. Land cover can be defined as the biophysical state of the Earth's surface and immediate subsurface, including biota, soil, topography, surface and ground water, and human structures (Turner *et al.* 1995). In other words, it describes both natural and man-made coverings of the Earth's surface. Land use can be defined as the human use of the land. Land use involves both the manner in which the biophysical attributes of the land are manipulated and the purpose for which the land is used (Turner *et al.* 1995). The relationship between land use and land cover is not always direct and obvious (Weng 1999). A single class of land cover may support multiple uses, while a single land use may involve the maintenance of several distinct land covers.

Urban areas are composed of a variety of materials, including different types of artificial materials (concrete, asphalt, metal, plastic, glass, etc.), soils, rocks, minerals, and green and non-photosynthetic vegetation. Remote sensing technology has often been applied to map land use or land cover, instead of materials. Each type of land cover may possess unique surface properties (materials); however, mapping land cover and mapping materials involves different requirements. Land cover mapping needs to consider characteristics in addition to those that come from the materials (Herold *et al.* 2006). The surface structure (roughness) may influence the spectral response as much as the intra-class variability (Gong and Howarth 1990, Myint 2001, Shaban and Dikshit 2001, Herold *et al.* 2006). Two different types of land cover, for example asphalt roads and composite shingle/tar roofs, may have very similar materials (hydrocarbons) and thus are difficult to discern, although from a materials perspective these surfaces can be mapped accurately with hyperspectral remote sensing techniques (Herold *et al.* 2006). Therefore, land cover

mapping requires taking into account the intra-class variability and spectral separability. Nevertheless, analysis of land use classes would be almost impossible with spectral information alone. Additional information, such as spatial, textural and contextual information, is usually required for successful land use classification in urban areas (Gong and Howarth 1992, Stuckens *et al.* 2000, Herold *et al.* 2003). The relationship between remote sensing of urban material, land cover and land use is illustrated in figure 2.

Traditional classification methods of LU/LC based on detailed fieldwork suffer two major common drawbacks: confusion between land use and land cover, and the lack of uniformity or comparability in classification schemes. These drawbacks make it difficult to compare land use patterns over time or between areas (Mather 1986). The use of aerial photographs and satellite images introduced in the late 1960s did not solve these problems because these techniques are based on the formal expression of land use rather than on the actual activity itself (Mather 1986). In fact, many land use types cannot be identified from the air. As a result, mapping of the Earth's surface tends to present a mixture of land use and land cover data with the emphasis on the latter (Lo 1986). This problem is reflected in the title of the classification developed in the USA for the mapping of the country at a scale of 1 : 100 000 or 1 : 250 000, commencing in 1974 (Anderson *et al.* 1976). Moreover, the United States Geological Survey (USGS) LU/LC Classification System has been designed as a resource-oriented system. Therefore, eight out of nine in the first-level categories relate to non-urban areas. The 2001 National Land-Cover Database developed by the USGS reflects both problems (Homer *et al.* 2004). Alternative to the USGS scheme, the Land-Based Classification Standard developed by the American Planning Association puts emphasis on extracting urban/suburban land use information. The parcel-level land use information is obtained from *in situ* surveys, aerial photography and high-resolution satellite imagery, based on the characteristics of activity, function, site development, structure and ownership

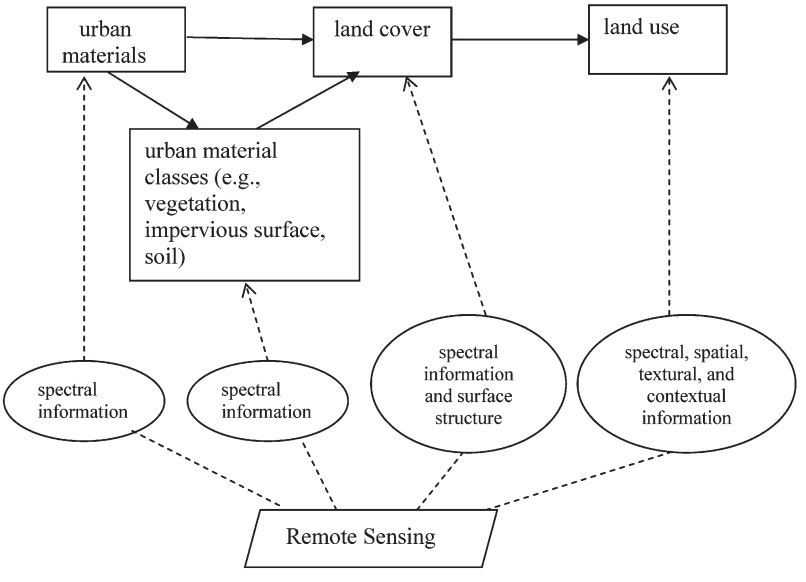

Figure 2. Relationship among remote sensing of urban materials, land cover and land use: a conceptual framework.

(American Planning Association 2004). In general, the success of most land use or land cover mapping is typically measured by the ability to match remote sensing spectral signatures to the Anderson classification scheme, which, in urban areas, is mainly land use (Ridd 1995). The confusion between land use and land cover contributes to the low classification accuracy (Foody 2002), while less emphasis on land cover in urban areas weakens the ability of digital remote sensing as a research tool for characterizing and quantifying the urban ecological structure and process (Ridd 1995).

2.1.2 The scale issue. The Anderson classification scheme was designed for use with remote sensing data, originally with aerial photography, at various scales and resolutions (Campbell 1983). However, the spatial scale and categorical scale are not explicitly linked in the classification scheme. The former refers to the manner in which image information content is determined by spatial resolution and the way the spatial resolution is handled in the image processing, while the latter refers to the level of detail in classification categories (Ju *et al.* 2005). This disconnection leads to the problem of simply lumping classes into more general classes in multiscale LU/LC classifications, which may cause a considerable loss of categorical information. As most classifications are conducted at a single spatial and categorical scale, there remains an important issue of matching an appropriate categorical scale of the Anderson scheme with the spatial resolution of the satellite image used (Welch 1982, Jensen and Cowen 1999). However, the nature of some applications requires LU/LC classification to be conducted at multiple spatial and/or categorical scales because a single scale cannot delineate all classes on account of the contrasting sizes, shapes and internal variations of different landscape patches (Wu and David 2002, Raptis *et al.* 2003). This is especially true for complex, heterogeneous landscapes, such as urban ecosystems. Moreover, when statistical clusters are grouped into LU/LC classes, in which smaller areas (e.g. pixels) are combined into larger ones (e.g. patches), both spatial resolution and statistical information are lost (Clapham 2003).

2.1.3 The image 'scene models'. Strahler *et al.* (1986) defined H- and L-resolution scene models based on the relationship between the size of the scene elements and the resolution cell of the sensor. The scene elements in the L-resolution model are smaller than the resolution cells, and are therefore not detectable. When the objects in the scene become much smaller than the resolution cell size, they may no longer be regarded as objects individually. Hence, the reflectance measured by the sensor may be treated as a sum of interactions among various types of scene elements as weighted by their relative proportions (Strahler *et al.* 1986). This is what happens with medium-resolution satellite imagery, such as those of Landsat TM or ETM+, Advanced Spaceborne Thermal Emission and Reflection Radiometer (ASTER), Satellite Pour l'Observation de la Terre (SPOT) and Indian satellites, applied to urban mapping. As the spatial resolution interacts with the fabric of urban landscapes, the problem of mixed pixels is created. Such a mixture becomes especially prevalent in residential areas, where buildings, trees, lawns, concrete and asphalt can all occur within a pixel (Epstein *et al.* 2002). Mixed pixels have been recognized as a major problem in the effective use of remotely sensed data in LU/LC classification and change detection (Fisher 1997, Cracknell 1998). The low accuracy of LU/LC classification in urban areas reflects, to a certain degree, the inability of traditional per-pixel classifiers, such as the maximum-likelihood classifier, to handle composite signatures.

2.2 *Landscape as a continuum*

2.2.1 The conceptual view. The prevalent problem of mixed pixels in urban remote sensing is that the instantaneous field of the view of the medium-resolution sensors does not match the operational scale of the landscapes. Such landscapes are better viewed as a continuum formed by continuously varying proportions of idealized materials, just as soils may be described in terms of the proportions of sand, silt and clay (Mather 1999). Agricultural land in the Midwest USA, residential areas and semi-arid areas are typical examples of continuum-type landscapes. Ridd's V-I-S model is a continuum model for urban areas in semi-arid land. Although the V-I-S model has demonstrated usefulness for characterizing and quantifying urban landscape patterns, its use in practice is still constrained by the following factors. First, the V-I-S model cannot explain all land cover types such as water and wetlands. Second, an impervious surface is difficult to identify as a single surface material or material class (Wu and Murray 2003, Lu and Weng 2006*a*,*b*). Third, the distinction between soils and impervious surfaces may not be easy in multispectral remote sensing imagery. In addition, Ridd's statistical sampling method for deriving the V, I and S components has high subjectivity, and may not be representative of the whole urban landscape. The data used were from colour infrared photographs at the scale of 1 : 30 000. To apply this conceptual model to digital remote sensing data, it is necessary to use digital image processing algorithms and techniques. Previous studies have attempted to relate the V-I-S model to various remote sensing data, but its linkage with advanced computational algorithms has been less seriously explored. In this paper we apply the V-I-S concept for a spatial–temporal analysis of the urban morphology in Indianapolis with LSMA, and by doing so, the potentials and limitations of this model for characterizing and quantifying urban landscape components can be examined further.

2.2.2 LSMA. The mathematical model of LSMA can be expressed as:

$$R_i = \sum_{k=1}^{n} f_k R_{ik} + E_i \tag{1}$$

where $i=1, \ldots, m$ (number of spectral bands); $k=1, \ldots, n$ (number of endmembers); R_i is the spectral reflectance of band i of a pixel that contains one or more endmembers; f_k is the proportion of endmember k within the pixel; R_{ik} is the known spectral reflectance of endmember k within the pixel in band i; and E_i is the error for band i. To solve f_k, the following conditions must be satisfied: (1) selected endmembers should be independent of each other, (2) the number of endmembers should not be larger than the spectral bands used, and (3) selected spectral bands should not be highly correlated. A constrained least-squares solution assumes that the following two conditions are satisfied simultaneously:

$$\sum_{k=1}^{n} f_k = 1 \tag{2}$$

and $0 \leqslant f_k \leqslant 1$

$$\mathrm{RMSE} = \sqrt{\left(\sum_{i=1}^{m} E_i^2 \Big/ m\right)} \tag{3}$$

where RMSE is the root mean square error for band i. The estimation of endmember

fraction images involves four steps: image processing, endmember selection, unmixing solution, and evaluation of fraction images. Of these steps, selecting suitable endmembers is the most important one in the development of high-quality fraction images. Two types of endmembers can be applied: image endmembers and reference endmembers. The former are derived directly from the image itself, while the latter are derived from field measurements or the laboratory spectra of known materials (Roberts *et al.* 1998). Many remote sensing applications have used image endmembers because they can be easily obtained and are capable of representing the spectra measured at the same scale as the image data (Roberts *et al.* 1998). Image endmembers can be derived from the extremes of the image feature space, based on the assumption that they represent the purest pixels in the image (Boardman 1993).

3. Study area

The city of Indianapolis, located in Marion County, Indiana, with a population of over 800 000, was chosen as the study area (figure 3). It is a key centre of manufacturing, warehousing, distribution and transportation. Situated in the middle of the country, Indianapolis possesses several other advantages that make it an appropriate choice. It has a single central city, and other large urban areas in the vicinity have not influenced its growth. The city is located on a flat plain and is relatively symmetrical, having possibilities of expansion in all directions. Like most American cities, Indianapolis is increasing in population and in area. The areal expansion is through encroachment into the adjacent agricultural and non-urban land. Certain decision-making forces, such as density of population, distance to

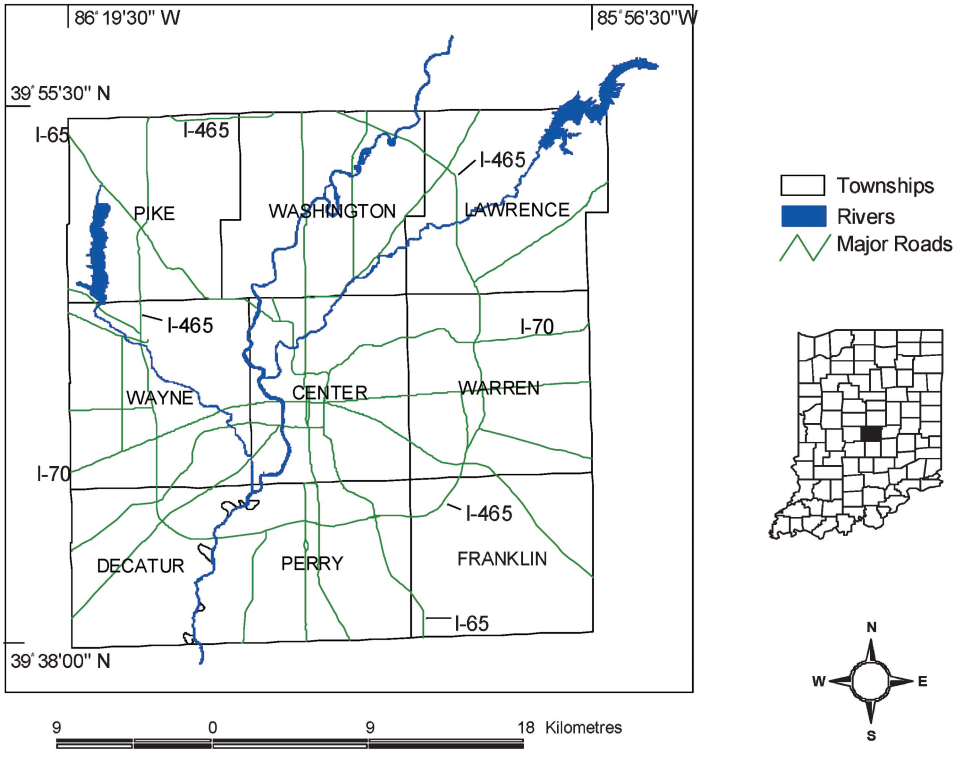

Figure 3. Study area: City of Indianapolis, Indiana, USA.

work, property value and income structure, encourage some sectors of metropolitan Indianapolis to expand faster than others. Examining its urban landscape patterns and dynamics is conducive to understanding and planning its future development.

4. Data and methods

4.1 *Image preprocessing*

Landsat TM images of 6 June 1991 (acquisition time: approximately 1045 h) and 3 July 1995 (approximately 1028 h) and a Landsat ETM + image of 22 June 2000 (approximately 1114 h) were used in this study. Although the images purchased were geometrically corrected, the geometrical accuracy determined was not high enough for combining them with other high-resolution data sets. The images were therefore further rectified to a common Universal Transverse Mercator (UTM) coordinate system based on 1 : 24 000 scale topographic maps, and were resampled to a pixel size of 30 m for all bands using the nearest-neighbour algorithm. An RMSE of less than 0.2 pixels was obtained for all the rectifications. These Landsat images were acquired under clear-sky conditions, and an improved image-based dark object subtraction model was applied to implement atmospheric corrections (Chavez 1996, Lu *et al.* 2002).

4.2 *Image endmember development*

To identify image endmembers effectively and to achieve high-quality endmembers, different image transform approaches, such as principal component analysis (PCA) and minimum noise fraction (MNF), can be applied to transform the multispectral images into a new data set (Green *et al.* 1988, Boardman and Kruse 1994). In this research, image endmembers were selected from the feature spaces formed by the MNF components (Garcia-Haro *et al.* 1996, Cochrane and Souza 1998, van der Meer and de Jong 2000, Small 2001, 2002, 2004). The MNF transform contains two steps: (1) decorrelation and rescaling of the noise in the data based on an estimated noise covariance matrix, producing transformed data in which the noise has unit variance and no band-to-band correlations; and (2) implementation of a standard PCA of the noise-whitened data. The result of the MNF transform is a two-part dataset, one part associated with large eigenvalues and coherent eigenimages, and a complementary part with near-unity eigenvalues and noise-dominated images (ENVI 2000). By performing an MNF transform, noise can be separated from the data by saving only the coherent portions, thus improving the spectral processing results. In this research, the MNF procedure was applied to transform the Landsat ETM + (the 2000 image) six reflective bands into a new coordinate set. The first three MNF components accounted for the majority of the information (99%) and were used for the selection of endmembers. The scatterplots between the MNF components are illustrated in figure 4(*a*), showing the potential endmembers. Four endmembers, namely green vegetation, high-albedo, low-albedo and soil, were finally selected. Figure 4(*b*) shows spectral reflectance characteristics of the selected endmembers. Next, a constrained least-square solution was applied to unmix the six ETM + reflective bands into four fraction images. The same procedures were used for derivation of fraction images from the Landsat TM 1991 and 1995 images. The first three MNF components computed from the 1991 and 1995 images also accounted for more than 99% of the scene variance, and the topologies of the triangular mixing space were consistent with that shown in figure 4(*a*). Figure 5 shows four fraction images for the three years.

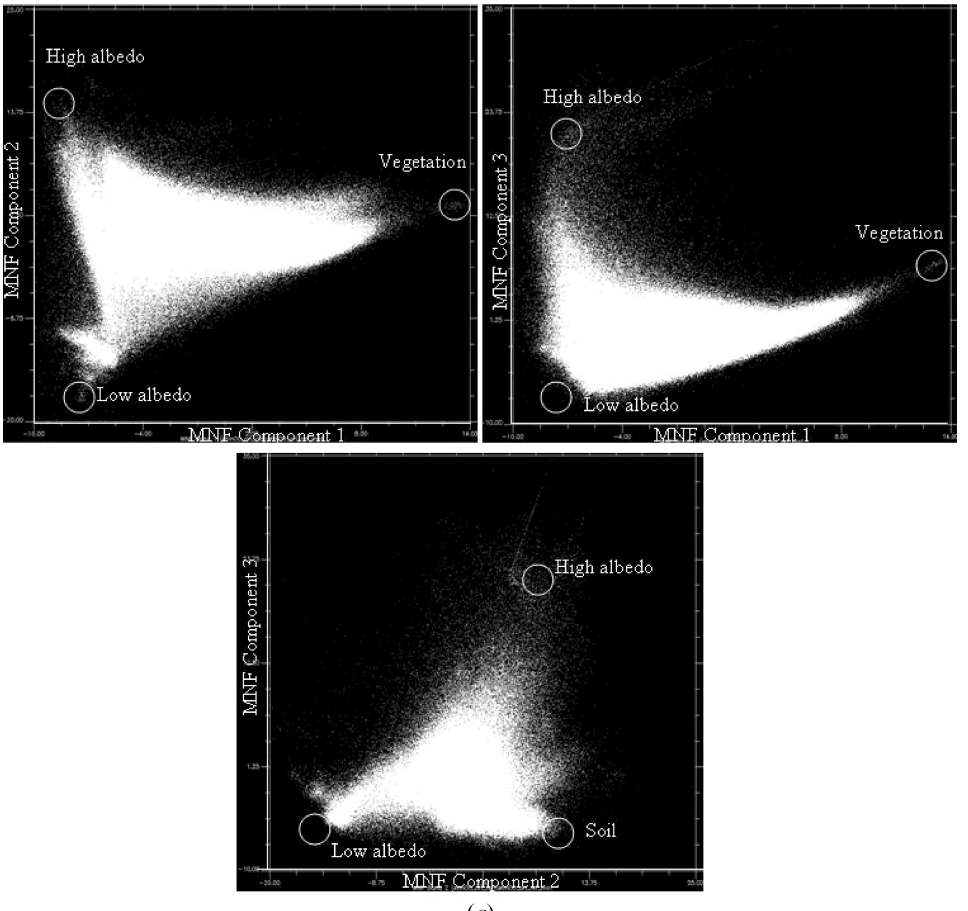

(*a*)

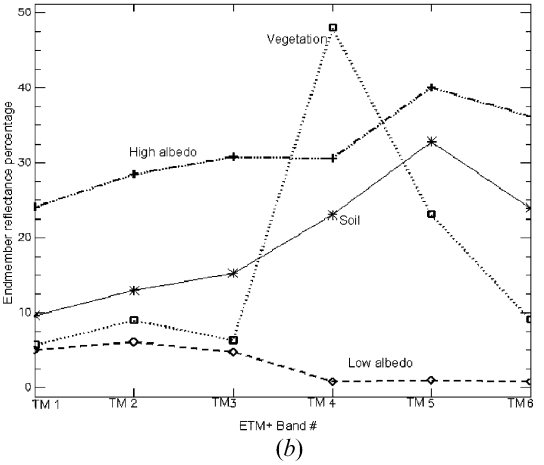

(*b*)

Figure 4. (*a*) Feature spaces between the MNF components, illustrating potential endmembers of Landsat ETM + image. (*b*) Spectral reflectance characteristics of the selected endmembers.

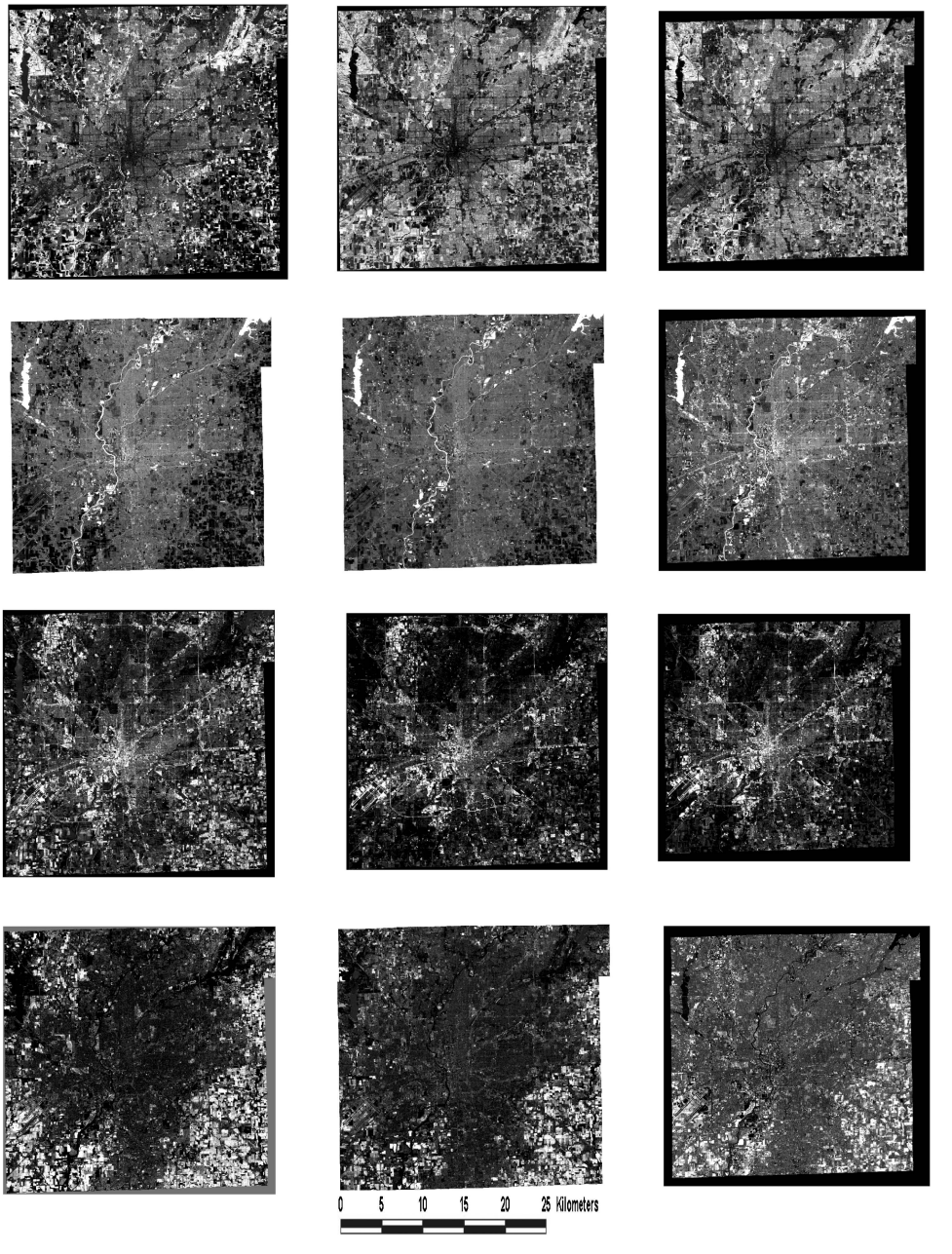

Figure 5. Fraction images from spectral mixture analysis of each year: first column, 1991; second column, 1995; third column, 2000; first row, green vegetation; second row, low albedo; third row, high albedo; fourth row, soil.

4.3 *Extraction of impervious surfaces*

Previous research has indicated that impervious surfaces can be computed by adding the high- and low-albedo fractions (Wu and Murray 2003), but this method did not consider the impact of pervious surfaces on the low- and high-albedo fraction

images, which often resulted in overestimation of impervious surfaces. Our experiment with Landsat ETM + imagery indicates that although the high-albedo fraction image related mainly to impervious surface information such as buildings and roads, it also related to other land cover such as dry soils. However, the low-albedo fraction image was found to be associated with water and shadows, such as water body, shade from forest canopy and tall buildings, and moisture in crops or pastures. Some impervious surfaces, especially dark impervious surfaces, were also linked to the low-albedo fraction image. Therefore, it is important to develop a suitable analytical procedure for the removal of non-impervious information from the fraction images. In this study, we developed a procedure by using land surface temperature data to isolate non-impervious from impervious surfaces and using soil fraction images as the thresholds to purify the high-albedo fraction images (figure 6).

For the high-albedo fraction images, impervious surfaces were predominantly confused with dry soils. Therefore, the soil fraction images can be used to remove soils from the high-albedo fraction images. For the low-albedo fraction images, dark impervious surfaces were confused with water and shadows. Therefore, the crucial step was to separate impervious surfaces from non-impervious pixels, including water, vegetation (forest, pasture, grass and crops) and soils. The following expert rules were used in this study:

(1) If the pixel values in the land surface temperature image are $\leqslant$t1, pixels in low- and high-albedo fraction images would be assigned to 0, otherwise pixel values in low- and high-albedo fraction images would be kept.
(2) If the pixel values in the soil fraction image are $>$t2, pixels in high-albedo fraction images would be assigned to 0, otherwise pixel values in the high-albedo fraction images would be kept.

In these rules, the t1 and t2 thresholds were identified based on reference data for water, vegetation and soils. After non-impervious pixels were removed from the

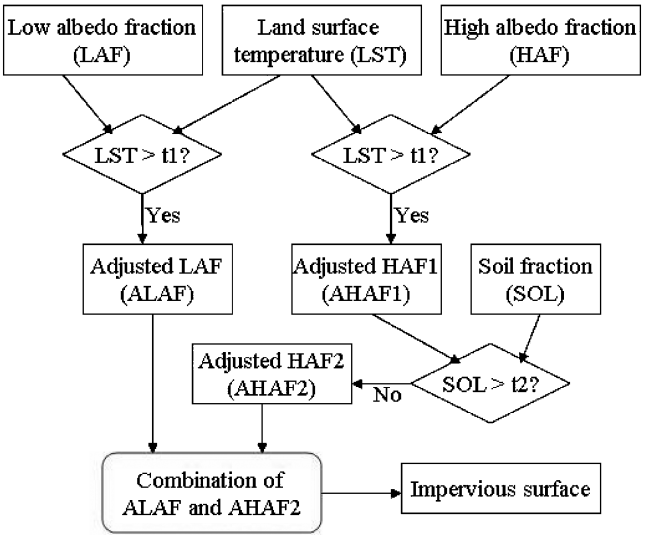

Figure 6. Flow-chart showing the procedures for developing an impervious surface image.

low- and high-albedo fraction images, the impervious surface image was developed by the addition of adjusted low- and high-albedo fraction images. Figure 7 presents a comparison of the impervious surface images before and after the adjustment. Our accuracy assessment of the Landsat ETM + image resulted in an overall RMSE of 9.22% and a system error of 5.68% (Lu and Weng 2006*a*).

4.4 *Image classification*

Fraction images were used for thematic land classification through a hybrid procedure that combined maximum-likelihood and decision-tree classifiers (Lu and Weng 2004). Sample plots were identified from high-resolution aerial photographs, initially covering 10 LU/LC types: commercial and industrial, high-density residential, low-density residential, bare soil, crop, grass, pasture, forest, wetland, and water. On average, between 10 and 16 sample plots were selected for each class. A window size of three by three was applied to extract the fraction value for each plot. The mean and standard deviation values were calculated for each LU/LC class. The characteristics of fractional composition for selected LU/LC types were then examined. Next, the maximum-likelihood classification algorithm was applied to classify the fraction images into 10 classes, generating a classified image and a distance image. A distance threshold was selected for each class to screen out the pixels that probably do not belong to that class, which was determined by examining interactively the histogram of each class in the distance image. Pixels with a distance value greater than the threshold were assigned a class value of zero. A decision-tree classifier was then applied to reclassify these pixels. The parameters required by the decision-tree classifier were identified based on the mean and standard deviation of the sample plots for each class. Finally, the accuracy of each classified image was checked with a stratified random sampling method (Jensen 2005) against the reference data for 150 samples collected from large-scale aerial photographs. This sampling method allows for various numbers of samples to be selected from each category of LU/LC, depending on the complexity of that category (Jensen 2005). To simplify the urban landscape analysis, 10 classes were merged into six LU/LC types: (1) commercial and industrial urban land, (2) residential land, (3) agricultural and pasture land, (4) grassland, (5) forest and (6) water (Lu and Weng 2004). Table 1 presents the definitions of the LU/LC categories.

5. Results

5.1 *Urban morphological analysis based on the V-I-S model*

The three images in the first row of figure 4 shows the geographic patterns of green vegetation (GV) fractions. These images display a large dark area (low fraction values) at the centre of the study area corresponding to the central business district of Indianapolis City. Bright areas of high GV values were found in the surrounding areas. Various types of crops were still at the early stage of growth or were before emergence, as indicated by the medium grey to dark tone of the GV fraction images in the southeastern and southwestern parts of the city. Table 2 shows that forest had the highest GV fraction values, followed by grassland. By contrast, commercial and industrial land displayed the lowest GV values. A low vegetative amount was found in water bodies, as indicated by the GV fraction values. Both residential land and pasture/agricultural land yielded a medium GV fraction value, subject to the impact of the dates of image acquired. In all the years observed, pasture/agricultural land

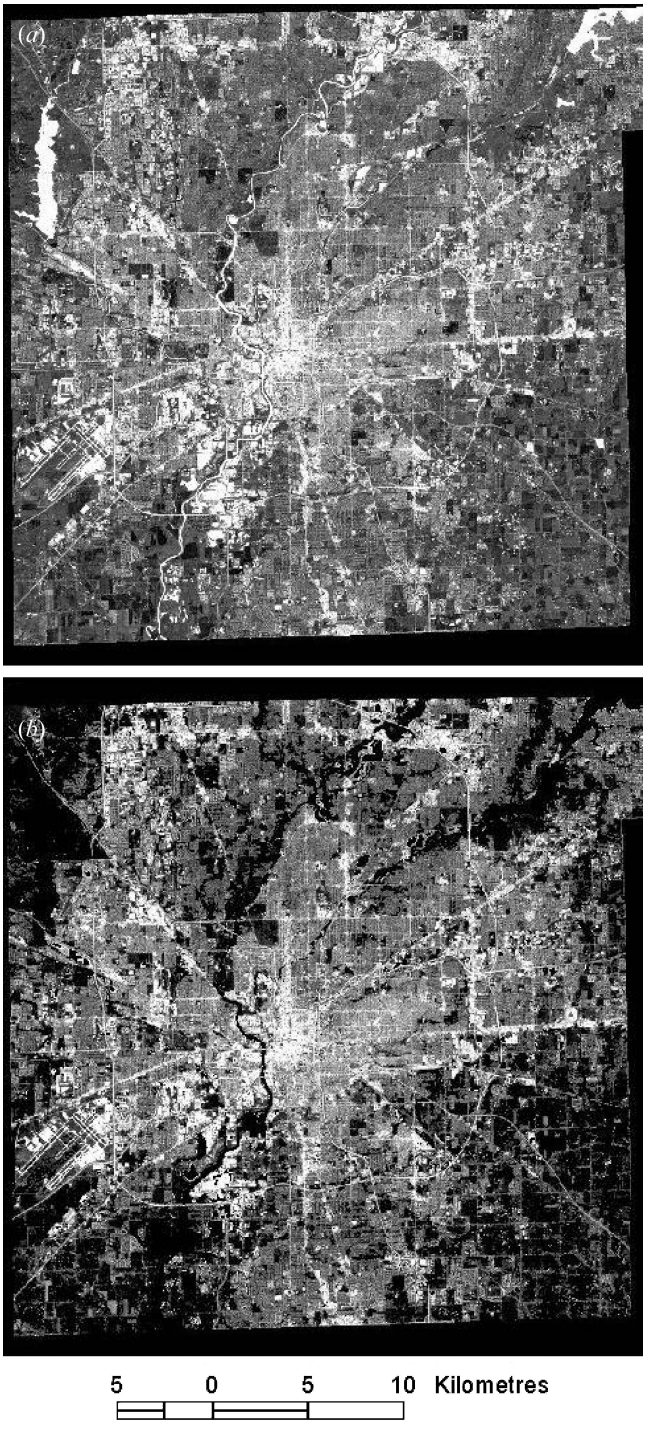

Figure 7. Comparison of impervious surface images developed from different methods. The image values range from 0 to 1, with lowest values in black and highest values in white. (*a*) Based on the direct addition of high- and low-albedo fraction images; (*b*) based on the addition of modified high- and low-albedo fraction images, in which other cover types were removed in the impervious surface image through the combined use of land surface temperature and fraction images.

Table 1. Description of the LU/LC categories.

Category	Descriptions
Urban land	The areas that have a high percentage (⩾30%) of impervious surfaces, such as asphalt, concrete and buildings. This category includes commercial, industrial and transportation. Barren lands are also included.
Residential land	Areas that typically have 25–75% of impervious surfaces, mixed with grass, trees, water, and so on. There are 16 categories of residential use in the study area. Information on each zoning category, typical density, primary use, minimum open space, typical lot size, and comprehensive planning classification was provided to the authors by the Metropolitan Planning Department, City of Indianapolis.
Forest land	The areas characterized by tree cover (natural or semi-natural woody vegetation), including natural deciduous forest, evergreen forest, mixed forest, urban and suburban forest, and shrubs.
Grasslands	Urban/recreational grasses planted in developed settings for recreation, erosion control or aesthetic purposes, such as parks, lawns, golf courses, airport grasses and industrial site grasses.
Pasture and agricultural land	Row crop by type, cereal grains, vineyards, feedlots, residue management, and confined operations. Also includes the areas covered by herbaceous vegetation including pasture/hay planted for livestock grazing or the production of hay.
Water	All areas of open water, including lake, rivers and streams, ponds, and outdoor swimming pools.

exhibited a large standard deviation value, suggesting that pasture and agricultural land may hold various amount of vegetation.

The percentage of land covered by impervious surfaces may vary significantly with LU/LC categories and subcategories (Soil Conservation Service 1975). This study shows a substantially different estimate for each LU/LC type, as a spectral unmixing model was applied to the remote sensing images, and the modelling had introduced some errors, as expected. For example, a high impervious fraction value was found in water because water was related to the low albedo fraction, and the latter was included in the computation of impervious surface. In general, an LU/LC type with a higher GV fraction appeared to have a lower impervious fraction. Commercial and industrial land detected very high impervious fraction values of around 0.7 in all years. Residential land came next with fraction values around 0.5. Grassland, pasture/agricultural land and forestland detected lower values of impervious surface largely because of their exposed bare soil, confusion with commercial/industrial and residential land, and modelling errors.

Soil fraction values were generally low in the majority of the urban area, but high in the surrounding areas. In particular, in agricultural fields located in the southeastern and southwestern parts of the city, soil fraction images appeared very bright because various types of crops were still at the early stage of growth. Table 2 shows that pasture/agricultural land showed a fraction value close to 0.4 at all times. Grassland possessed medium fraction values averaging 0.25, substantially higher than the fraction values of forestland and residential land. Commercial and industrial land displayed similar fraction values as grassland, which had much to do with its confusion with dry soils in the high-albedo images. Water generally

Table 2. V-I-S compositions of LU/LC types in Indianapolis in 1991, 1995 and 2000.

	1991 TM image			1995 TM image			2000 ETM+image		
Land cover type	Vegetation	Impervious surface	Soil	Vegetation	Impervious surface	Soil	Vegetation	Impervious surface	Soil
Commercial and industrial	0.167	0.709	0.251	0.127	0.679	0.273	0.125	0.681	0.276
	(0.128)	(0.190)	(0.193)	(0.097)	(0.178)	(0.177)	(0.092)	(0.205)	(0.191)
Residential	0.314	0.558	0.198	0.371	0.508	0.149	0.298	0.467	0.247
	(0.132)	(0.138)	(0.152)	(0.115)	(0.108)	(0.092)	(0.095)	(0.124)	(0.137)
Grassland	0.433	0.451	0.268	0.553	0.366	0.155	0.442	0.276	0.305
	(0.176)	(0.135)	(0.208)	(0.145)	(0.096)	(0.131)	(0.099)	(0.083)	(0.119)
Agriculture and pasture	0.304	0.374	0.602	0.388	0.291	0.378	0.371	0.275	0.407
	(0.213)	(0.112)	(0.285)	(0.191)	(0.091)	(0.236)	(0.168)	(0.072)	(0.222)
Forest	0.654	0.436	0.182	0.716	0.388	0.046	0.584	0.327	0.175
	(0.162)	(0.128)	(0.166)	(0.085)	(0.065)	(0.052)	(0.075)	(0.074)	(0.055)
Water	0.226	0.730	0.188	0.176	0.805	0.094	0.111	0.891	0.078
	(0.186)	(0.197)	(0.178)	(0.210)	(0.167)	(0.068)	(0.120)	(0.136)	(0.071)

Values given as mean (standard deviation).

possessed a minimal impervious fraction value. Like the GV fraction, the soil fraction displayed the highest standard deviation values in pasture/agricultural land because of the various amount of emerging vegetation.

When mean signature values of the fractions for each LU/LC type are plotted, quantitative relationships among the thematic LU/LC types in terms of the V-I-S composition can be examined. Figure 8 shows the V-I-S composition by LU/LC in each year, with an area delineating one standard deviation from the mean fraction value.

5.2 *Landscape change and the V-I-S dynamics*

The fraction images were classified into three thematic maps, as shown in figure 9. Overall accuracy, producer's accuracy and user's accuracy were calculated based on the error matrix for each classified map, as well as the KHAT statistic, kappa variance and Z statistic. The overall accuracies of the LU/LC maps for 1991, 1995 and 2000 were determined to be 90%, 88% and 89%, respectively. Thus, LU/LC data derived from the LSMA procedure have a reasonably high accuracy, and are sufficient for urban landscape analysis. Taking the 2000 ETM + image as an example, a comparison of LSMA-based image classification performance with MLC of all multispectral bands of the same image was conducted. Table 3 shows the error matrices for the two classified images. A significant improvement (9%) was found with the LSMA-based image classification method.

Table 4 shows the composition of LU/LC by year and the changes that occurred between two time intervals. In 1991, residential use and pasture/agriculture accounted equally for 27% of the total land, while grassland shared another 20%. The combination of commercial and industrial land used 13% of the total area, and forestland had a close match, yielding another 10%. Water bodies occupied the remaining 3%, and this percentage was unchanged from 1991 to 2000. However, LU/LC dynamics occurred in all other categories, as seen in the last three columns of table 4. The most notable increment was observed in residential use, which changed from 27% in 1991 to 33% in 1995, reaching 38% in 2000. Associated with this change, grassland increased from 20% to 23%. Highly developed land, mainly for commercial and industrial use, transportation and utilities, continued to expand. In 2000, it accounted for >15 000 ha, or 15%, generating a 2% increase over the 9 years. These results suggest that urban land dispersal in Indianapolis was related both to population increase and to economic growth. By contrast, a pronounced decrease in pasture and agricultural land was found from 1991 (27%) to 1995 (20%). This decrease was also evident between 1995 and 2000, when pasture and agricultural land decreased further by 6581.30 ha (31.56%). Forestland in a city like Indianapolis was understandably limited in size. Our remote sensing geographic information system (GIS) analysis indicates, however, that forestland continued to disappear with a stable, marked rate. Between 1991 and 2000, forestland was reduced by 2864.81 ha (i.e. 28.75%), levelling down to approximately 7100 ha. The cross-tabulation of the 1991 and 2000 LU/LC maps reveals that most of the losses in pasture, agricultural and forestland were due to conversion to residential and other urban uses, following the continued process of urbanization and suburbanization. GIS overlay of the two maps further shows the spatial occurrence of urban expansion to be mostly at the edges of the city. These changes in LU/LC have led to changes in the composition of image fractions.

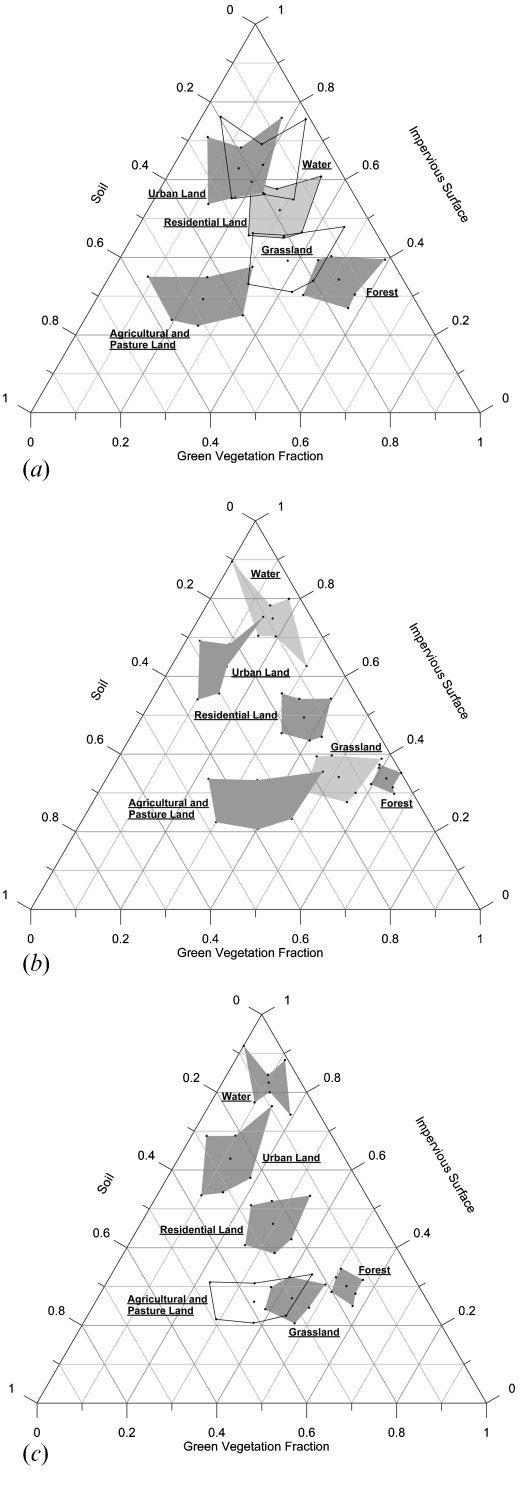

Figure 8. Quantitative relationships among the LU/LC types with respect to the V-I-S model: (*a*) 1991; (*b*) 1995; (*c*) 2000.

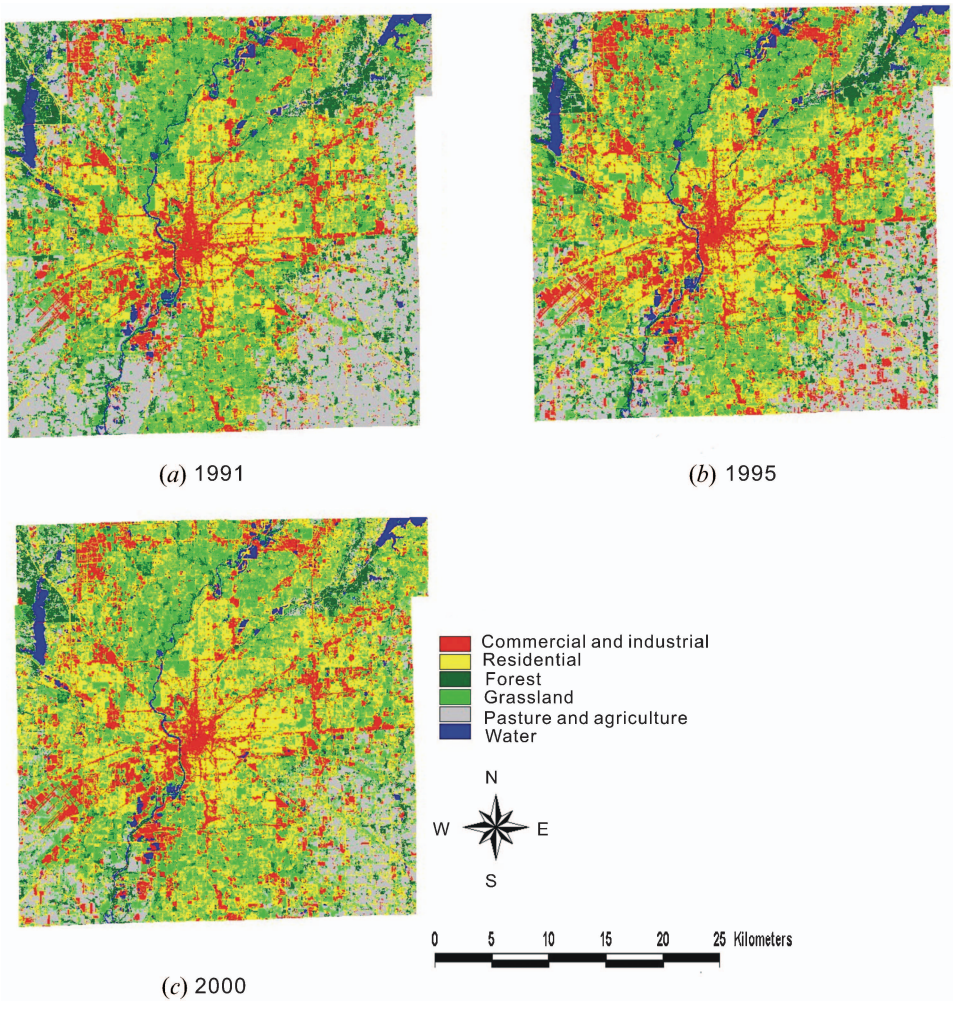

Figure 9. LU/LC maps of (*a*) 1991, (*b*) 1995 and (*c*) 2000.

Impervious surface, as an important urban land cover feature, not only indicates the degree of urbanization but also is a major contributor to the environmental impact of urbanization (Arnold and Gibbons 1996). To examine how impervious surfaces in Indianapolis had changed from 1991 to 2000, figure 10 was created to show the distribution of impervious surfaces for the observed years at four categories. Table 5 shows that the amount of pixels with values greater than zero increased from 42 501 in 1991 to 45 804 in 1995, and further increased to 46 560 in 2000. A comparison between 1991 and 2000 indicates that this increase in the amount of pixels took place over the entire range of impervious fraction values (except for the category of 0.1–0.2). This analysis further substantiates the above findings, that is that Indianapolis underwent an extensive urbanization process, during which impervious or impenetrable surfaces, such as rooftops, roads, parking lots, driveways and sidewalks, were widely generated. In other words, a significant amount of non-urban pixels became urbanized during the study period. Furthermore, in 1991, only 7.03% of the urbanized pixels (pixels that contain some

Table 3. A comparison of image classification accuracy between the spectral mixture analysis (SMA)-based classifier and the maximum likelihood classifier (MLC).

Method	Classified data	Reference data						Reference total	Classified total	Number correct	Producer's accuracy (%)	User's accuracy (%)	Kappa
		Urban	Residential	Forest	Grass	Pasture and agricultural	Water						
SMA	Urban	21	0	0	0	1	0	26	22	21	80.77	95.45	0.945
	Residential	3	56	0	1	2	0	57	62	56	98.25	90.32	0.844
	Forest	0	0	9	0	0	0	11	9	9	81.82	100.00	1.000
	Grass	0	1	1	28	1	0	32	31	28	87.50	90.32	0.877
	Pasture and agricultural	2	0	1	3	16	0	20	22	16	80.00	72.73	0.685
	Water	0	0	0	0	0	4	4	4	4	100.00	100.00	1.000
	Overall classification accuracy=89.33% (i.e. 134/150), overall Kappa statistics=0.8575												
MLC	Urban	19	1	0	0	1	0	26	21	19	73.08	90.48	0.885
	Residential	7	56	0	7	2	0	57	72	56	98.25	77.78	0.642
	Forest	0	0	8	0	0	0	11	8	8	72.73	100.00	1.000
	Grass	0	0	3	18	2	0	32	23	18	56.25	78.26	0.724
	Pasture and agricultural	0	0	0	7	15	0	20	22	15	75.00	68.18	0.633
	Water	0	0	0	0	0	4	4	4	4	100.00	100.00	1.000
	Overall classification accuracy=80.00% (i.e. 120/150), overall Kappa statistics=0.7284												

Variance for SMA=0.001115; variance for MLC=0.001923; Z statistic=2.342654; significant at 98% confidence level.

Table 4. Changes in land use and land cover in Indianapolis, 1991–2000.

	Area (ha)			Change in area (ha, % in parentheses)		
LU/LC type	1991	1995	2000	1991–1995	1995–2000	1991–2000
Commercial and industrial	13 322.10	16 706.50	15 489.00	3384.40 (25.40)	−1217.50 (−7.29)	2166.90 (16.27)
Residential	28 708.90	34 123.70	40 771.70	5414.80 (18.86)	6648 (19.48)	12 062.80 (42.02)
Grassland	21 132.50	21 356.60	23 976.40	224.10 (1.06)	2619.80 (12.27)	2843.90 (13.46)
Pasture and agricultural	28 466.00	20 853.80	14 272.50	−7612.20 (−26.74)	−6581.30 (−31.56)	−14 193.50 (−49.86)
Forest	9965.58	8547.71	7100.77	−1417.87 (−14.23)	−1446.94 (−16.93)	−2864.81 (−28.75)
Water	2894.21	2903.96	2903.06	9.75 (0.34)	−0.90 (−0.03)	8.85 (0.31)

impervious surface areas) had a value of impervious fraction greater than 0.6. In 1995 and 2000, these values were 7.41% and 9.24%, respectively. This increase in pixel counts in the higher percentage categories of the impervious fraction suggests that even more construction had taken place in previously urbanized pixels, that is, there existed an infill type of urban development (Wilson *et al.* 2003).

5.3 *Intra-urban variations and the V-I-S compositions*

The intra-urban variations of landscape structures can be examined by a comparative analysis of the V-I-S compositions of each township in the city, based on the mean and standard deviation values of vegetation, impervious surface and soil by LULC type for each township. The computation results show that each LU/LC had a distinct V-I-S composition pattern but it was fairly consistent over the three dates of observation, implying relatively small changes in the V-I-S composition for each land class. A further comparison of the V-I-S mean values of six LU/LC classes for the nine townships shows that the composition was generally stable, with slight changes, for the three observed years. For commercial and industrial land of any township, the mean value of vegetation was around 0.15, the impervious surface close to 0.7, and soil a little over 0.25. For residential land, the mean values of the V-I-S components for each township were found to be approximately 0.3, 0.5 and 0.2, respectively. These patterns of V-I-S composition appear similar to the characteristics of the V-I-S composition pattern for the whole city, as indicated in table 3.

The disparity in the V-I-S composition in the townships can be revealed by plotting and examining in detail the mean values and changes in the V, I and S components with ternary diagrams. Figure 11 shows the changes in V-I-S compositions (mean fraction values) by LU/LC type by township from 1991 to 2000. By focusing our analysis on the V-I-S composition of commercial/industrial and residential lands, some interesting observations can be made. The two townships Pike and Decatur experienced continued development in commercial/industrial land during the study period. This development had resulted in an increase in the I component but a decrease in the V component, while the S component largely remained constant over time. The trend of commercial development in these townships was heading along the interstate highways such as I-65, I-465 and I-70, converting large areas of forest and agricultural land into impervious surfaces. Figures 11(*a*) and 11(*g*) further show that commercial/industrial land was moving away from residential land. This implies that commercial activities did not occur within (or near) the residential areas. Urban development in these areas may be characterized as urban fringe expansion, linear and leapfrog clustered development. In the Center and Washington Townships, not much change occurred in the I component, as shown in figures 11(*e*) and 11(*b*), because these townships had been fully developed in the past. The decrease in the V component and the increase in the S component were probably associated with an infill type of development or redevelopment activities. This urbanization pattern was characterized by the development of vacant land in already built-up areas and/or redevelopment of abandoned industries, warehouses and other types of old buildings, which usually occurred in the places where public facilities already existed (Forman 1995). In contrast to the above two types of urban development, the Franklin Township in the southeastern part of the city exhibited another type of development, which can be called clustered, or leap-frog, development. The urban

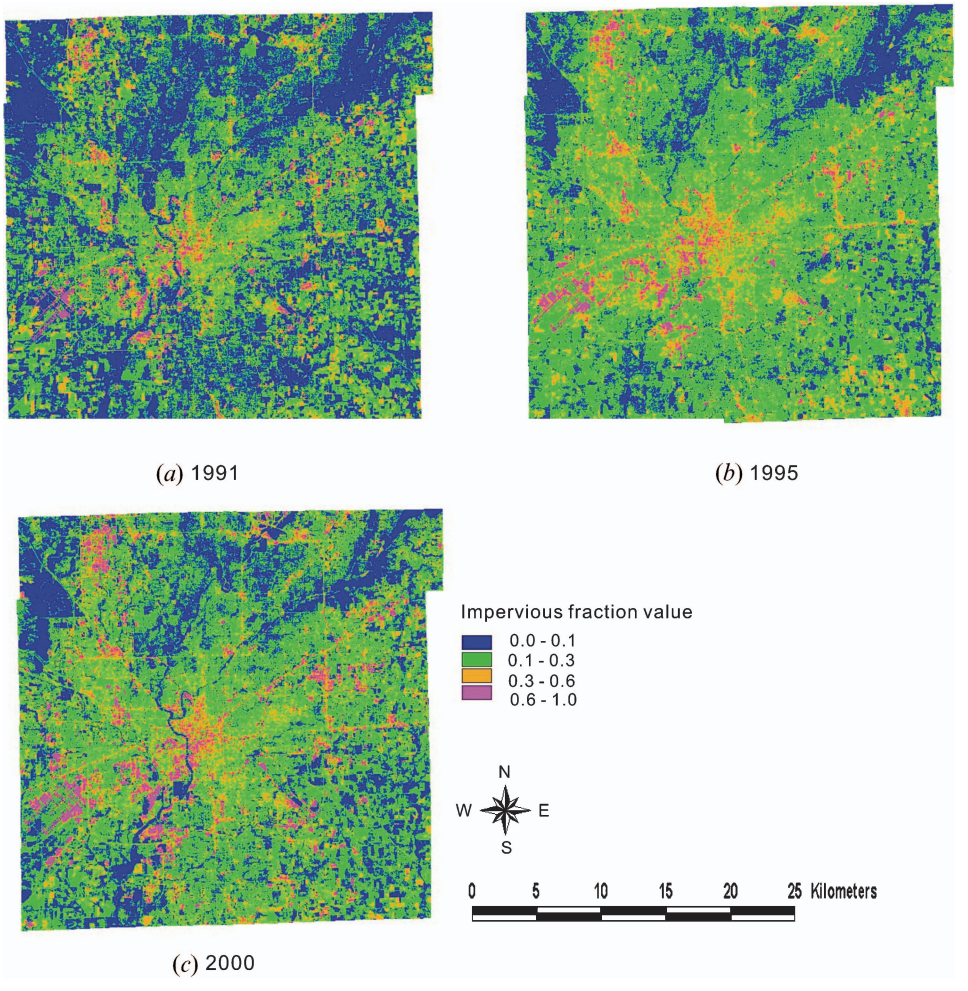

Figure 10. Distribution of impervious coverage by year: (*a*) 1991; (*b*) 1995; (*c*) 2000.

development in Franklin typically involved compact, high-density development of functionally separated clusters. The ternary plot in figure 11(*i*) shows that the pattern of V-I-S composition has not become stabilized for the periods observed. Commercial development was largely introduced into the residential areas, especially after 1995. Residential and commercial lands thus appeared increasingly intermingled. The remaining four townships, Wayne, Perry, Lawrence and Warren, did not discover urban growth as distinct as the above townships. Instead, urban development in these areas displayed some sort of combination of fringe development, infill development and outlying growth. The latter can be defined as the development beyond existing developed areas, and may be broken down into isolated, linear branch and clustered branch (Wilson *et al.* 2003). Ternary plots (*c*), (*d*), (*f*) and (*h*) in figure 11 show that that the I component in commercial land altered over the time, but might have experienced the opposite direction of change between the periods 1991–1995 and 1995–2000. The changes in impervious surfaces inevitably triggered changes in the vegetation and soil components, leading to the V-I-S dynamics. These dynamics can also be clearly observed in the residential land.

Table 5. Number of pixels (those containing some impervious surface) in each percentage category of impervious surface.

Impervious fraction value	Pixel counts		
	1991	1995	2000
$\leqslant 0.1$	1355	1373	1823
$\leqslant 0.2$	17 880	17 350	17 300
$\leqslant 0.3$	9630	12 080	12 010
$\leqslant 0.4$	6904	7485	7276
$\leqslant 0.5$	3743	4121	3850
$\leqslant 0.6$	1459	1751	1961
$\leqslant 0.7$	781	810	1106
$\leqslant 0.8$	406	414	651
$\leqslant 0.9$	215	269	347
$\leqslant 1.0$	128	151	236
Total	42 501	45 804	46 560

6. Discussion and conclusions

Remote sensing of urban material, land use and land cover has different requirements. This study aimed to examine their relationship by using a continuum

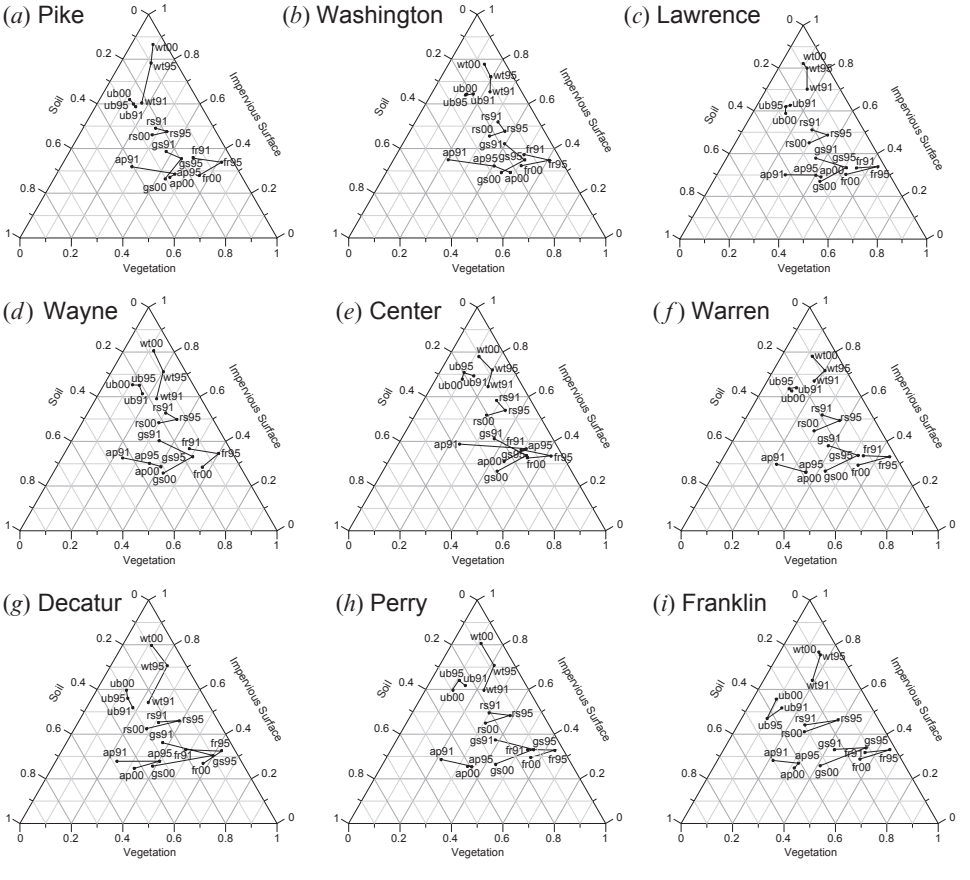

Figure 11. Changes in the V-I-S composition by LU/LC type by township.

field model. This model was developed based on the reconciliation of the V-I-S model (Ridd 1995) and LSMA of Landsat imagery. The case study demonstrated successfully that the continuum model was effective for characterizing and quantifying the spatial and temporal changes of the landscape compositions in Indianapolis between 1991 and 2000.

The linkage between Ridd's model and LSMA lies in the urban material. Ridd (1995) suggested that urban landscape can be decomposed into three classes of urban materials (vegetation, impervious surfaces and soil) but did not implement the model using digital image processing algorithms. LSMA has been widely used to analyse spectrally heterogeneous urban reflectance based on 'endmembers', which are recognizable surface materials that have homogeneous spectral properties over the entire image. The number of endmembers that can be extracted from a satellite image is determined by the data dimensionality reflected in the image mixing space, which, in turn, is subject to the number of spectral bands available. Theoretically, Landsat TM/ETM + images, with six spectral bands (excluding the thermal infrared band), can derive as many as seven endmembers. However, our study indicated that the three lower-order principal components accounted for more than 99% of the image variance, indicating that the mixing space was perfectly three-dimensional. The RMSE was small (less than 0.1 of mean pixel reflectance) for all three unmixings. Therefore, the endmembers selected for this study (high albedo, low albedo, vegetation and soil) were regarded as suitable to account for the observed radiance. When high- and low-albedo endmembers were used to model impervious surfaces, the RMSE was also found to be reasonably small for the LSMA models (<0.02). As such, LSMA with the four-endmember model offered a simple, robust, physically based solution to quantify the urban reflectance. Our study further indicated that, although spectral endmembers were different over the time because of changes in urban materials and LU/LC, the topology of the triangular mixing space (figure 4) was consistent. It became apparent that LSMA can provide a repetitive way to derive consistent image endmembers from Landsat images. Therefore, by representing Ridd's V-I-S components as image fractions, the continuum model develop in this study provided an effective approach for quantifying urban landscape patterns as standardized component surfaces.

The V-I-S image fractions can be used not only for characterizing urban morphology and biophysical conditions but also for LU/LC classification. The classifications based on the image fractions would be able to accommodate the spectral heterogeneity that characterizes the urban landscape in medium-resolution imagery. By contrast, with the 'hard' classifiers, each thematic class is assumed to be both spatially and spectral homogeneous at the pixel scale (Small 2005). Moreover, the continuum variables that LSMA provided can more accurately characterize the 'fuzzy' nature of the urban landscapes. Fuzzy classification intends to address this fuzzy nature but does not provide a physical solution for the urban reflectance (Small 2004). This study further shows that, statistically, LSMA-derived fractions can be used to generate better classification results. Stable and reliable fraction estimates derived from the multitemporal image data were found to be straightforward for an analysis of urban landscape dynamics because the fractional characteristics of LULC types at one date were comparable with other dates of fraction estimates. Many digital change detection methods for urban growth analysis use pixel-by-pixel comparison algorithms, which may cause the problem of error propagation in the overlay process. Compared to other urban growth models

based on multitemporal remote sensing imagery (e.g. Batty and Longley 1994, Clarke and Gaydos 1998, Auch *et al.* 2004), this continuum model offers a more flexible way for urban time–space modelling and comparison of urban morphologies in different geographical settings because it took into account the physical process responsible for the observed radiance and provided a more accurate representation of urban landscapes. It should be noted that the images used in this study were close to the anniversary date and atmospheric correction was conducted using an improved image-based calibration approach for these images. However, relative radiometric correction was not performed so that the spectral reflectance of an individual band at one date cannot be directly related to that at other dates. The V-I-S fractions derived from LSMA, which used transformed MNF component images, were based on the spectral relationship among the image bands of the same date. Our fieldwork proved that these fraction values and their changes over time were sensible.

The V-I-S model has been applied successfully to both temperate (Salt Lake City, Columbus, Ohio, Indianapolis, Los Angeles, USA; Queensland, Australia; Cairo, Egypt; Shanghai, China) and tropical cities (Bangkok, Thailand; Yogyakarta, Indonesia; Manaus, Brazil) under different climate conditions. A main strength of the V-I-S model lies in its generalization and simplification of urban land cover into the components of vegetation, impervious surface and soil. The 'soil' in the model may include various types of soils, bare ground and sparsely vegetated areas. The 'vegetation' refers to green vegetation, and may include trees, grasses, pastures, crops, and so on. Both 'vegetation' and 'soil' may have distinct seasonal variability, while impervious surface is relatively stable. Urban mapping must consider the daily, seasonal and annual phenological cycles of vegetation, which affect the temporal pattern of soil. In addition to the temporal variability, the spectral variability of the V-I-S components must be addressed. For instance, because of the complexity of impervious surfaces, different urban areas may have substantially different types of impervious surfaces. Identifying a single endmember to represent all types of impervious surfaces may not be realistic. This study shows that the impervious surface was overestimated in less-developed areas but underestimated in well-developed areas. Impervious surface may have highly similar spectral responses with non-photosynthesis vegetation and dry soils. On the contrary, shade from tall buildings, large tree crowns and dark objects may cause impervious surfaces to be underestimated. The limitation in the spectral resolution of Landsat imagery makes it impractical to derive and depict various types of impervious surfaces with several endmembers. To overcome this problem, a multiple-endmember LSMA model has been developed and found to be more effective when a large number of endmembers are required to be modelled across an image scene (Painter *et al.* 1998, Roberts *et al.* 1998, Okin *et al.* 2001, Powell *et al.* 2007). In addition, calibration with reference endmembers from a spectral library or *in situ* measurements would also be desirable.

The spectral variability of the vegetation fraction is another significant issue in LSMA of Landsat imagery for urban landscapes (Song 2005). Our study indicated that the vegetation endmember usually corresponded to grass or dense crops or pasture. Because forest possessed an internal shade component, it was located along the mixing line between the vegetation and low-albedo endmembers. Shade is an important component captured by optical remote sensors, and was therefore included in the Lu–Weng model (Lu and Weng 2004). Impervious surface, shade and vegetation were considered to be three basic components in the urban areas,

while in the surrounding areas, soil, vegetation and shade were used to account for the spectral variability. However, the Lu–Weng 2004 model was not able to separate soil and impervious surface materials. In this study, low- and high-albedo endmembers were derived to depict better the impervious surface. Low-albedo endmembers were found to mainly correspond to water, canopy shade, tall building shade, or dark impervious surface materials. Future studies should refine this endmember and examine how it is related to shade, water and other materials.

The spatial variability of the V-I-S model also needs to be examined. The intra-urban variability is a consequence of the wide variety of urban materials, land cover and land use in different parts of the city. Our investigation of the V-I-S dynamics in the nine townships of Indianapolis due to changes in the urban landscape revealed an urban-to-rural gradient in these components. This explains the effectiveness of the continuum model for such an urban growth analysis. The concept of 'urban' and 'city' was not differentiated well in the Ridd's study. We suggest that, based on previous studies, the V-I-S model may be extended to the land cover of cities (including urban, suburban and surrounding rural areas). Wu *et al.* (2005) suggested that different V-I-S models should be constructed for different functional districts. The inter-urban variability results from the diversity of biophysical, geological, economical, social and urban development history among cities. Small (2005) compared 28 cities in the world, and found that these cities had a similar mixing topology in Landsat ETM+imagery and can be represented by three-component (high-albedo, dark, and vegetation endmembers) linear mixture models in both scene-specific and global composite mixing spaces. This current research could be extended in the future by testing the hypothesis that the Indianapolis model can only be applied to cities in developed countries and not to cities in developing countries. The model can be parameterized and validated for certain time periods of selected cities using available medium-resolution satellite data. The results of our model applied to and parameterized for developed countries can then be compared with those for developing countries, with the aim of developing a global model for remotely sensed analysis of urban landscapes.

Acknowledgements

This research was supported by the National Science Foundation (BCS-0521734) in a project entitled 'Role of urban canopy composition and structure in determining heat islands: a synthesis of remote sensing and landscape ecology approach'. We thank the anonymous reviewers for their constructive comments and suggestions.

References

ADAMS, J.B., SABOL, D.E., KAPOS, V., FILHO, R.A., ROBERTS, D.A., SMITH, M.O. and GILLESPIE, A.R., 1995, Classification of multispectral images based on fractions of endmembers: application to land cover change in the Brazilian Amazon. *Remote Sensing of Environment*, **52**, pp. 137–154.

ADAMS, J.B., SMITH, M.O. and JOHNSON, P.E., 1986, Spectral mixture modeling: a new analysis of rock and soil types at the Viking Lander site. *Journal of Geophysical Research*, **91**, pp. 8098–8112.

AGUIAR, A.P.D., SHIMABUKURO, Y.E. and MASCARENHAS, N.D.A., 1999, Use of synthetic bands derived from mixing models in the multispectral classification of remote sensing images. *International Journal of Remote Sensing*, **20**, pp. 647–657.

AMERICAN PLANNING ASSOCIATION, 2004, *Land-Based Classification System* (Washington, DC: American Planning Association). Available online at: www.planning.org/lbcs/ (accessed 20 January 2007).

ANDERSON, J.R., HARDY, E.E., ROACH, J.T. and WITMER, R.E., 1976, *A Land Use and Land Cover Classification System for Use with Remote Sensor Data*. US Geological Survey Professional Paper 964 (Washington, D.C.: US Government Printing Office).

ARNOLD, C.L., JR. and GIBBONS, C.J., 1996, Impervious surface coverage: the emergence of a key environmental indicator. *Journal of the American Planning Association*, **62**, pp. 243–258.

ASNER, G.P. and LOBELL, D.B., 2000, A biogeophysical approach for automated SWIR unmixing of soils and vegetation. *Remote Sensing of Environment*, **74**, pp. 99–112.

AUCH, R., TAYLOR, J. and ACEVEDO, W., 2004, *Urban Growth in American Cities: Glimpses of U.S. Urbanization*. U.S. Geological Survey Circular 1252, US Department of the Interior.

BETTY, M. and LONGLEY, P., 1994, *Fractal Cities* (San Diego, CA: Academic Press).

BOARDMAN, J.W., 1993, Automated spectral unmixing of AVIRIS data using convex geometry concepts. In *Summaries of the Fourth JPL Airborne Geoscience Workshop*, JPL Publication 93-26, pp. 11–14 (Pasadena, CA: NASA Jet Propulsion Laboratory).

BOARDMAN, J.W. and KRUSE, F.A., 1994, Automated spectral analysis: a geological example using AVIRIS data, north Grapevine Mountains, Nevada. *Proceedings, ERIM Tenth Thematic Conference on Geologic Remote Sensing*, 9–12 May 1994, Ann Arbor, MI, pp. 407–418 (Ann Arbor, MI: Enviromental Research Institute of Michigan).

BOARDMAN, J.M., KRUSE, F.A. and GREEN, R.O., 1995, Mapping target signature via partial unmixing of AVIRIS data. In *Summaries of the Fifth JPL Airborne Earth Science Workshop*, JPL Publication 95-1, NASA Jet Propulsion Laboratory, Pasadena, CA, pp. 23–26.

CAMPBELL, J.B., 1983, *Mapping the Land: Aerial Imagery for Land Use Information* (Washington, DC: Association of American Geographers).

CHAVEZ, P.S., JR., 1996, Image-based atmospheric corrections – revisited and improved. *Photogrammetric Engineering and Remote Sensing*, **62**, pp. 1025–1036.

CLAPHAM, W.B., JR., 2003, Continuum-based classification of remotely sensed imagery to describe urban sprawl on a watershed scale. *Remote Sensing of Environment*, **86**, pp. 322–340.

CLARKE, K.C. and GAYDOS, L.J., 1998, Loose-coupling a cellular automaton model and GIS: long-term urban growth prediction for San Francisco and Washing/Baltimore. *International Journal of Geographic Information Science*, **12**, pp. 699–714.

COCHRANE, M.A. and SOUZA, C.M., JR., 1998, Linear mixture model classification of burned forests in the eastern Amazon. *International Journal of Remote Sensing*, **19**, pp. 3433–3440.

CRACKNELL, A.P., 1998, Synergy in remote sensing – what's in a pixel? *International Journal of Remote Sensing*, **19**, pp. 2025–2047.

ENVI, 2000, *ENVI User's Guide* (Boulder, CO: Research Systems Inc.).

EPSTEIN, J., PAYNE, K. and KRAMER, E., 2002, Techniques for mapping suburban sprawl. *Photogrammetric Engineering and Remote Sensing*, **63**, pp. 913–918.

FISHER, P., 1997, The pixel: a snare and a delusion. *International Journal of Remote Sensing*, **18**, pp. 679–685.

FOODY, G.M., 2002, Status of land cover classification accuracy assessment. *Remote Sensing of Environment*, **80**, pp. 185–201.

FORMAN, R.T.T., 1995, *Land Mosaics: The Ecology of Landscapes and Regions* (Cambridge: Cambridge University Press).

GARCIA-HARO, F.J., GILABERT, M.A. and MELIA, J., 1996, Linear spectral mixture modeling to estimate vegetation amount from optical spectral data. *International Journal of Remote Sensing*, **17**, pp. 3373–3400.

GONG, P. and HOWARTH, P.J., 1990, The use of structure information for improving land-cover classification accuracies at the rural–urban fringe. *Photogrammetric Engineering and Remote Sensing*, **56**, pp. 67–73.

GONG, P. and HOWARTH, P.J., 1992, Frequency-based contextual classification and gray-level vector reduction for land-use identification. *Photogrammetric Engineering and Remote Sensing*, **58**, pp. 423–437.

GREEN, A.A., BERMAN, M., SWITZER, P. and CRAIG, M.D., 1988, A transformation for ordering multispectral data in terms of image quality with implications for noise removal. *IEEE Transactions on Geoscience and Remote Sensing*, **26**, pp. 65–74.

HEROLD, M., LIU, X. and CLARK, K.C., 2003, Spatial metrics and image texture for mapping urban land use. *Photogrammetric Engineering and Remote Sensing*, **69**, pp. 991–1001.

HEROLD, M., SCHIEFER, S., HOSTERT, P. and ROBERTS, D.A., 2006, Applying imaging spectrometry in urban areas. In *Urban Remote Sensing*, Q. Weng and D. Quattrochi (Eds), pp. 137–161 (Boca Raton, FL: CRC/Taylor & Francis).

HOMER, C., HUANG, C., YANG, L., WYLIE, B. and COAN, M., 2004, Development of a 2001 national land-cover database for the United States. *Photogrammetric Engineering and Remote Sensing*, **70**, pp. 829–840.

JENSEN, J.R., 2005, *Introductory Digital Image Processing: A Remote Sensing Perspective* (Upper Saddle River, NJ: Pearson Prentice Hall).

JENSEN, J.R. and COWEN, D.C., 1999, Remote sensing of urban/suburban infrastructure and socio-economic attributes. *Photogrammetric Engineering and Remote Sensing*, **65**, pp. 611–622.

JU, J., GOPAL, S. and KOLACZYK, E.D., 2005, On the choice of spatial and categorical scale in remote sensing land cover classification. *Remote Sensing of Environment*, **96**, pp. 62–77.

LEE, S. and LATHROP, R.G., JR., 2005, Sub-pixel estimation of urban land cover components with linear mixture model analysis and Landsat Thematic Mapper imagery. *International Journal of Remote Sensing*, **26**, pp. 4885–4905.

LO, C.P., 1986, *Applied Remote Sensing* (New York: Longman Inc).

LU, D., MAUSEL, P., BRONDIZIO, E. and MORAN, E., 2002, Assessment of atmospheric correction methods for Landsat TM data applicable to Amazon basin LBA research. *International Journal of Remote Sensing*, **23**, pp. 2651–2671.

LU, D. and WENG, Q., 2004, Spectral mixture analysis of the urban landscapes in Indianapolis with Landsat ETM+imagery. *Photogrammetric Engineering and Remote Sensing*, **70**, pp. 1053–1062.

LU, D. and WENG, Q., 2006*a*, Use of impervious surface in urban land use classification. *Remote Sensing of Environment*, **102**, pp. 146–160.

LU, D. and WENG, Q., 2006*b*, Spectral mixture analysis of ASTER imagery for examining the relationship between thermal features and biophysical descriptors in Indianapolis, Indiana. *Remote Sensing of Environment*, **104**, pp. 157–167.

MADHAVAN, B.B., KUBO, S., KURISAKI, N. and SIVAKUMAR, T.V.L.N., 2001, Appraising the anatomy and spatial growth of the Bangkok Metropolitan area using a vegetation-impervious-soil model through remote sensing. *International Journal of Remote Sensing*, **22**, pp. 789–806.

MATHER, A.S., 1986, *Land Use* (London: Longman).

MATHER, P.M., 1999, Land cover classification revisited. In *Advances in Remote Sensing and GIS*, P.M. Atkinson and N.J. Tate (Eds), pp. 7–16 (New York: John Wiley & Sons).

MCGWIRE, K., MINOR, T. and FENSTERMAKER, L., 2000, Hyperspectral mixture modeling for quantifying sparse vegetation cover in arid environments. *Remote Sensing of Environment*, **72**, pp. 360–374.

MYINT, S.W., 2001, A robust texture analysis and classification approach for urban land-use and land-cover feature discrimination. *Geocarto International*, **16**, pp. 27–38.

OKE, T.R., 1982, The energetic basis of the urban heat island. *Quarterly Journal of the Royal Meteorological Society*, **108**, pp. 1–24.

OKIN, G.S., ROBERTS, D.A., MURRAY, B. and OKIN, W.J., 2001, Practical limits on hyperspectral vegetation discrimination in arid and semiarid environments. *Remote Sensing of Environment*, **77**, pp. 212–225.

PHINN, S., STANFORD, M., SCARTH, P., MURRAY, A.T. and SHYY, P.T., 2002, Monitoring the composition of urban environments based on the vegetation-impervious surface-soil (VIS) model by subpixel analysis techniques. *International Journal of Remote Sensing*, **23**, pp. 4131–4153.

POWELL, R.L., ROBERTS, D.A., DENNISON, P.E. and HESS, L.L., 2007, Sub-pixel mapping of urban land cover using multiple endmember spectral mixture analysis: Manaus, Brazil. *Remote Sensing of Environment*, **106**, pp. 253–267.

RAPTIS, V.S., VAUGHAN, R.A. and WRIGHT, G.G., 2003, The effect of scaling on land cover classification from satellite data. *Computers and Geosciences*, **29**, pp. 705–714.

RASHED, T., WEEKS, J.R., ROBERTS, D.A., ROGAN, J. and POWELL, R., 2003, Measuring the physical composition of urban morphology using multiple endmember spectral mixture models. *Photogrammetric Engineering and Remote Sensing*, **69**, pp. 1011–1020.

RASHED, T., WEEKS, J.R., STOW, D. and FUGATE, D., 2005, Measuring temporal compositions of urban morphology through spectral mixture analysis: toward a soft approach to change analysis in crowded cities. *International Journal of Remote Sensing*, **26**, pp. 699–718.

RIDD, M.K., 1995, Exploring a V-I-S (Vegetation-Impervious Surface-Soil) model for urban ecosystem analysis through remote sensing: comparative anatomy for cities. *International Journal of Remote Sensing*, **16**, pp. 2165–2185.

ROBERTS, D.A., BATISTA, G.T., PEREIRA, J.L.G., WALLER, E.K. and NELSON, B.W., 1998, Change identification using multitemporal spectral mixture analysis: applications in eastern Amazonia. In *Remote Sensing Change Detection: Environmental Monitoring Methods and Applications*, R.S. Lunetta and C.D. Elvidge (Eds), pp. 137–161 (Chelsea, MI: Ann Arbor Press).

SETIAWAN, H., MATHIEU, R. and THOMPSON-FAWCETT, M., 2006, Assessing the applicability of the V-I-S model to map urban land use in the developing world: case study of Yogyakarta, Indonesia. *Computers, Environment and Urban Systems*, **30**, pp. 503–522.

SHABAN, M.A. and DIKSHIT, O., 2001, Improvement of classification in urban areas by the use of textural features: the case study of Lucknow city, Uttar Pradesh. *International Journal of Remote Sensing*, **22**, pp. 565–593.

SMALL, C., 2001, Estimation of urban vegetation abundance by spectral mixture analysis. *International Journal of Remote Sensing*, **22**, pp. 1305–1334.

SMALL, C., 2002, Multitemporal analysis of urban reflectance. *Remote Sensing of Environment*, **81**, pp. 427–442.

SMALL, C., 2004, The Landsat ETM + spectral mixing space. *Remote Sensing of Environment*, **93**, pp. 1–17.

SMALL, C., 2005, A global analysis of urban reflectance. *International Journal of Remote Sensing*, **26**, pp. 661–681.

SOIL CONSERVATION SERVICE, 1975, *Urban Hydrology for Small Watersheds.* Technical Release No. 55 (Washington, DC: USDA Soil Conservation Service).

SONG, C., 2005, Spectral mixture analysis for subpixel vegetation fractions in the urban environment: how to incorporate endmember variability? *Remote Sensing of Environment*, **95**, pp. 248–263.

STRAHLER, A.H., WOODCOCK, C.E. and SMITH, J.A., 1986, On the nature of models in remote sensing. *Remote Sensing of Environment*, **70**, pp. 121–139.

STUCKENS, J., COPPIN, P.R. and BAUER, M.E., 2000, Integrating contextual information with per-pixel classification for improved land cover classification. *Remote Sensing of Environment*, **71**, pp. 282–296.

TURNER, B.L., II., SKOLE, D., SANDERSON, S., FISHER, G., FRESCO, L. and LEEMANS, R., 1995, *Land-Use and Land-Cover Change: Science and Research Plan.* IGBP Report No. 35 and HDP Report No. 7 (Stockholm and Geneva: International Geosphere-Bioshere Program and the Human Dimensions of Global Environmental Change Program).

VAN DER MEER, F. and DE JONG, S.M., 2000, Improving the results of spectral unmixing of Landsat Thematic Mapper imagery by enhancing the orthogonality of end-members. *International Journal of Remote Sensing*, **21**, pp. 2781–2797.

WANG, F., 1990, Fuzzy supervised classification of remote sensing images. *IEEE Transactions on Geoscience and Remote Sensing*, **28**, pp. 194–201.

WARD, D., PHINN, S.R. and MURRAY, A.T., 2000, Monitoring growth in rapidly urbanizing areas using remotely sensed data. *The Professional Geographer*, **53**, pp. 371–386.

WELCH, R.A., 1982, Spatial resolution requirements for urban studies. *International Journal of Remote Sensing*, **3**, pp. 139–146.

WENG, Q., 1999, *Environmental Impacts of Land Use and Land Cover Change in the Zhujiang Delta, China: An Analysis Using an Integrated Approach of GIS, Remote Sensing, and Spatial Modeling.* PhD dissertation, University of Georgia, Athens, Georgia.

WENG, Q., LU, D. and SCHUBRING, J., 2004, Estimation of land surface temperature-vegetation abundance relationship for urban heat island studies. *Remote Sensing of Environment*, **89**, pp. 467–483.

WILSON, E.H., HURD, J.D., CIVCO, D.L., PRISLOE, M.P. and ARNOLD, C., 2003, Development of a geospatial model to quantify, describe and map urban growth. *Remote Sensing of Environment*, **86**, pp. 275–285.

WU, C. and MURRAY, A.T., 2003, Estimating impervious surface distribution by spectral mixture analysis. *Remote Sensing of Environment*, **84**, pp. 93–505.

WU, J.G. and DAVID, J.L., 2002, A spatially explicit hierarchical approach to modeling complex ecological systems: theory and application. *Ecological Modelling*, **153**, pp. 7–26.

WU, J.G., JELINSKI, D.E., LUCK, M. and TUELLER, P.T., 2000, Multiscale analysis of landscape heterogeneity: scale variance and pattern metrics. *Geographic Information Sciences*, **6**, pp. 6–19.

WU, J.W., XU, J.H. and YUE, W.Z., 2005, V-I-S model for cities that are experiencing rapid urbanization and development. *Geoscience and Remote Sensing Symposium, IGARSS'05. Proceedings*, **3**, pp. 1503–1506.